# Surface Spin Waves in the Heisenberg Antiferromagnet with Changes in Exchange and Anisotropy Constants at the Surface

R. E. De Wames and T. Wolfram
*Science Center, North American Rockwell Corporation, Thousand Oaks, California 91360*

(Received 24 February 1969)

The dependence of the surface spin-wave eigenmodes on the ratio of the surface exchange to the bulk exchange $\epsilon_\perp$, and on the surface anisotropy energy for {100} surfaces of a bcc antiferromagnet is calculated. For $0 \leqslant \epsilon_\perp \leqslant 1$, we find two acoustic-type surface spin-wave branches associated with left-hand $+E$ and right-hand $-E$ circular polarization, both of which are lower in energy than the corresponding bulk modes. The $+E$ mode exists for all values of the two-dimensional propagation vector parallel to the surface, $\mathbf{k}$, which belong to the first Brillouin zone. The $-E$ acoustic surface-state branch is incomplete, being truncated at small $\mathbf{k}$, and has maximum excitation amplitude on the second layer of spins—in contrast to the above mentioned $+E$ branch, which has its maximum on the surface. The truncation of a surface branch occurs whenever decay into the bulk continuum states is possible. In the range $1 < \epsilon_\perp < 2$, we also find two surface-wave branches: a complete $+E$ acoustic branch which approaches the bulk curve as $\epsilon_\perp \to 2$, and also a $-E$ optical-type branch which is cut off at small $\mathbf{k}$. Finally, for $\epsilon_\perp > 2$, there are three surface spin-wave branches: $+E$ acoustic branch which is truncated at large $\mathbf{k}$, and complete $+E$ and $-E$ optical branches. The eigenvectors for these modes are also derived.

## I. INTRODUCTION

A STUDY of the surface spin-wave spectrum of a "free" {100} surface of the body-centered cubic (bcc) two-sublattice Heisenberg antiferromagnet was recently reported by Mills and Saslow.[1] They found a single excitation branch whose states are characterized by a propagation vector parallel to the surface $\mathbf{k}$ and by an exponential decrease of the excitation amplitude with increasing distance from the surface. The dispersion curve for this surface spin-wave branch has a maximum energy which is lower by a factor of 2 than that of the bulk-antiferromagnetic state with the same $\mathbf{k}$ (but with vanishing propagation vector normal to a {100} surface). The surface-state energy at $\mathbf{k}=0$, which was found to be lower than the bulk-antiferromagnetic resonance mode by a factor of $\sqrt{2}$ whenever the anisotropy energy $\hbar\omega_A$ is small compared to the exchange energy $\hbar\omega_e$, was also shown by a perturbation treatment to be insensitive to small changes in the surface exchange and anisotropy energies.

It is reasonable to suppose that the surface exchange and anisotropy fields acting on spins at the surface of an antiferromagnet can be different from those acting on the interior spins.[2] It is, therefore, important to determine what effect changes in these parameters have on the surface spin-wave spectrum. In this article, we report on a study of the nature of the surface spin-wave spectrum of the {100} surface of the bcc two-sublattice antiferromagnet for arbitrary changes in the nearest-neighbor (nn) surface exchange parameter, as well as arbitrary changes in the anisotropy field acting on the surface spins. The results of this study show that for a reduced surface exchange parameter, two acoustic-type surface spin-wave branches exist, both of which lie below the bulk. The first branch, the $+E$ branch (to which we assign a left-hand circular polarization), has its maximum excitation amplitude on the surface and corresponds to a generalization of the branch discussed by Mills and Saslow. The second branch, the $-E$ branch (right-hand circular polarization), has its maximum amplitude on the second layer of spins. This branch extends to the end of the first Brillouin zone, but is truncated at small $\mathbf{k}$. In the case that the ratio of the surface exchange to the bulk exchange $\epsilon_\perp$ lies between 1 and 2, the $+E$ acoustic branch exists over the entire Brillouin zone. The $-E$ acoustic branch does not exist, but a new $-E$ optical-type branch now appears which is truncated at small $\mathbf{k}$. In the case that $\epsilon_\perp$ exceeds 2, there exist three surface spin-wave branches: a $+E$ acoustic branch which exists for $\mathbf{k}=0$, but is truncated at larger $\mathbf{k}$, a complete $+E$ optical branch, and a complete $-E$ optical branch. The energies of the optical and acoustical surface modes depend strongly upon the surface exchange for finite $\mathbf{k}$. The $\mathbf{k}=0$ energy, however, is relatively insensitive to the value of $\epsilon_\perp$ and to changes in the surface anisotropy, whenever the bulk anisotropy energy is small compared to the bulk exchange energy.

In the case that the anisotropy energy is comparable to the exchange energy, we find even for $\epsilon_\perp = 1$, the case considered by Mills and Saslow, that the $+E$ acoustical branch is truncated for small values of $\mathbf{k}$ when the anisotropy energy at the surface exceeds its bulk value. Optical modes are also found in this case.

In Sec. II, we outline the theory and derive eigenvalue equations for the spin-wave surface states. Numerical results for the various surface spin-wave branches are given in Sec. III, and in Sec. IV the corresponding eigenvectors are examined. Discussion of the results and some conclusions are presented in Sec. V.

[1] D. L. Mills and W. M. Saslow, Phys. Rev. **171**, 488 (1968).
[2] R. E. De Wames and T. Wolfram, Phys. Rev. Letters **12**, 137 (1969).

## II. THEORY

### A. Equations of Motion

The Hamiltonian for a two-sublattice Heisenberg antiferromagnet can be written in the form

$$H_s=\sum_{i,\Delta} J(i,\, i+\Delta)\mathbf{S}_i^{(a)}\cdot\mathbf{S}_{i+\Delta}^{(b)} -\sum_i [g(i)\mu_B H_e+\omega_A(i)]S_{iz}^{(a)} +\sum_i [\omega_A(j)-g(j)\mu_B H_e]S_{jz}^{(b)}, \quad (1)$$

where $J(i,\, i+\Delta)$ is the exchange integral, taken to be positive, between a spin at the lattice site $\mathbf{R}_i$ and a nn at $\mathbf{R}_{i+\Delta}$. The anisotropy energy is $\omega_A$, and we have assumed that a spin on sublattice $a$ has its nn on sublattice $b$. The quantity $H_e$ is the external magnetic field, $\mu_B$ is the Bohr magneton, $g$ has the usual meaning, and $\mathbf{S}_j$ is the spin angular momentum operator on the $j$th atom. The sum over $\Delta$ is over nn only.

In order to determine the dispersion law and normal modes of the surface spin waves, we employ the equations of motion

$$i\frac{d}{dt}L_j(t)=[L_j(t),H_s(t)], \quad (2)$$

with

$$L_j(t)=S_{j,x}(t)+iS_{j,y}(t). \quad (3)$$

In the random-phase approximation (RPA), we can write

$$[L_j^{(a)},H_s]=-\sum_\Delta J(j,\, j+\Delta)\langle S_{z,\,j+\Delta}^{(b)}\rangle L_j^{(a)} +\langle S_{z,j}^{(a)}\rangle\sum_\Delta J(j,\, j+\Delta)L_{j+\Delta}^{(b)} +[\omega_H(j)+\omega_A(j)]L_j^{(a)}, \quad (4)$$

where we have set

$$\omega_H=g\mu_B H_e. \quad (5)$$

The symbol $\langle\cdots\rangle$ refers to the expectation value of the operator. (To obtain the commutator $[L_j^{(b)},H_s]$, we replace the superscript $(a)$ by $(b)$ and change the sign of $\omega_A$.) We now introduce the Fourier transform of $L_j(t)$:

$$L_j^{(\mu)}(t)=\int_{-\infty}^{-\infty} L_j^{(\mu)}(E')e^{-iE't}dE', \quad (6)$$

and further write

$$L_j^{(\mu)}(E')=\frac{1}{(N_s)^{1/2}}\sum_{\mathbf{k}} e^{i\mathbf{k}\cdot\rho_j^{(\mu)}}u_{x_j}^{(\mu)}(\mathbf{k},E'). \quad (7)$$

The number of atoms on the surface whose normal is chosen parallel to the $x$ axis is $N_s$, the vector $\boldsymbol{\varrho}_j$ is the projection of the position vector $\mathbf{R}_j$ onto the surface, and $x_j$ is the position along the normal to the surface. The superscript $\mu(\mu=a,\, b)$ indicates the sublattice. In Eq. (7), it is understood that $x_j$ refers to a surface possessing spins belonging to the $\mu$ sublattice, and $\mathbf{k}$ is a two-dimensional propagation vector parallel to the crystal surface. Using Eqs. (2), (4), (6), and (7), we obtain a set of algebraic equations for the variables $u_{x_j}^{(\mu)}(\mathbf{k},E')$. For the {100} bcc surface geometry,

$$E'u_{x_j}^{(a)}(k,E') =[-\sum_\Delta J(\mathbf{R}_j^{(a)};\,\mathbf{R}_j^{(a)}+\boldsymbol{\Delta})\langle S_z^{(b)}(\mathbf{R}_j^{(a)}+\boldsymbol{\Delta})\rangle +\omega_H(\mathbf{R}_j^{a})+\omega_A(\mathbf{R}_j^{(a)})]u_{x_j}^{(a)}(\mathbf{k},E') +\langle S_z^{(a)}(\mathbf{R}_j^{(a)})\rangle\sum_\Delta e^{i\mathbf{k}\cdot\Delta_{||}}J(\mathbf{R}_j^{(a)};\,\mathbf{R}_j^{(a)}+\boldsymbol{\Delta}) \times u_{x_j+\Delta_x}^{(b)}(\mathbf{k},E'). \quad (8)$$

Here, $\boldsymbol{\Delta}_{||}$ and $\boldsymbol{\Delta}_x$ are the components of the position vectors of the nn parallel to the surface and normal to the surface. [To obtain the equations for $u_{x_j}^{(b)}(\mathbf{k},E')$, we replace $(a)$ by $(b)$ and change the sign of $\omega_A$.] For the {100} geometry a surface spin has first neighbors within the crystal but not on the surface. The crystal spin structure consists of sheets parallel to the {100} surface with all spins on a sheet up or down. We assume the first layer (surface layer) to have spin up, and label the spin-up (odd) layers by $u_1$, $u_2$, $\cdots$, $u_N$. The second layer has spins down, and we label the spin-down (even) layers, starting from the second layer, by $v_1$, $v_2$, $v_3$, $\cdots$, $v_N$. Symbolically, we have

$$u_l=u_{x_j}^{(a)},\qquad v_l=u_{x_k}^{(b)}. \quad (9)$$

In what follows, we take the exchange between the surface spins and their interior nn to be $J_\perp$, and all other exchange parameters to be $J$. We assume $\omega_A(\mathbf{R}_j^{\mu})$ to be $\omega_A(1)$ for the surface and $\omega_A$ elsewhere. We assume that $\langle S_z^{a}\rangle=-\langle S_z^{b}\rangle=\langle S_z\rangle$ for all spins except the surface spins which we shall denote by $\langle S_z^{a}(1)\rangle$ and $\langle S_z^{b}(1)\rangle$ $[=-\langle S_z^{a}(1)\rangle]$. Finally, we assume that the $g$ factor is $g(1)$ for the surface and $g$ elsewhere.

In the model described above, the expectation value of the $z$ component of the surface spin is allowed to deviate from bulk value when $T>0$. However, in this paper only the $T=0$ dispersion curves are calculated.

We now have the supermatrix equation[3]

$$\begin{bmatrix}\mathbf{D}_N+\boldsymbol{\Delta}\mathbf{D}_N, & \mathbf{O}_N\\ \mathbf{B}_N & \mathbf{I}_N\end{bmatrix}\begin{bmatrix}\mathbf{V}_N\\ \mathbf{U}_N\end{bmatrix}=0, \quad (10)$$

where $\mathbf{O}_N$ is the nul matrix, $\mathbf{I}_N$ the identity matrix, and

$$\mathbf{D}_N=\begin{bmatrix} 2\cos\theta, & -1, & 0, & 0, & \cdots\\ -1, & 2\cos\theta, & -1, & 0, & \cdots\\ 0, & -1, & 2\cos\theta, & -1, & \cdots\\ 0, & 0, & -1, & 2\cos\theta, & \cdots\\ \cdots & \cdots & \cdots & \cdots & \cdots\\ \cdots & \cdots & \cdots & \cdots & \cdots\\ \cdots & \cdots & \cdots & \cdots & \cdots \end{bmatrix}, \quad (11)$$

[3] The supermatrix Eq. (10) is constructed by solving for $u_l$ in terms of $v_l$.

and

$$\mathbf{B}_N=\begin{bmatrix} \frac{d_{12}-\omega_1}{E-\omega_0+d_{11}}, & 0, & 0, & 0, & \cdots \\ \frac{-\omega_1}{E-\omega_0}, & \frac{-\omega_1}{E-\omega_0}, & 0, & 0, & \cdots \\ 0, & \frac{-\omega_1}{E-\omega_0}, & \frac{-\omega_1}{E-\omega_0}, & 0, & \cdots \\ 0, & 0, & \frac{-\omega_1}{E-\omega_0}, & \frac{-\omega_1}{E-\omega_0}, & \cdots \\ \cdots & \cdots & & & \cdots \\ \cdots & \cdots & \cdots & & \cdots \end{bmatrix}, \quad (12)$$

$$\omega_0=\omega_e+\omega_A, \quad \omega_e=8J\langle S_z\rangle, \quad E=E'-\omega_H,$$
$$\omega_1=\left(\frac{\omega_e}{2}\right)\lambda_k, \quad \lambda_k=\tfrac{1}{4}\sum_{\Delta_{||}} e^{ik\cdot\Delta_{||}},$$
$$-2\cos\theta=\frac{E^2-\omega_0^2}{\omega_1^2}+2, \quad d_{12}=(\tfrac{1}{2}\omega_e)\lambda_k(1-\epsilon_\perp^{(1)}), \quad (13)$$
$$\epsilon_\perp^{(1)}=\frac{J_\perp\langle S_z(1)\rangle}{J\langle S_z\rangle}.$$

For the model discussed earlier, the $\mathbf{\Delta D}_N$ matrix has only one element $-\Delta d$ defined by

$$\Delta d=\frac{E-\omega_0}{\omega_1^2}\left[d_{22}+\frac{(\omega_1+d_{21})(\omega_1-d_{21})}{E-\omega_0+d_{11}}-\frac{\omega_1^2}{E-\omega_0}\right], \quad (14)$$

with

$$d_{22}=(\tfrac{1}{2}\omega_e)(\epsilon_\perp^{(1)}-1), \quad d_{21}=(\tfrac{1}{2}\omega_e)\lambda_k(\epsilon_\perp-1),$$
$$d_{11}=(\tfrac{1}{2}\omega_e)(2-\epsilon_\perp)+\Delta\omega_A+\Delta\omega_H, \quad (15)$$
$$\Delta\omega_A=\omega_A-\omega_A(1), \quad \Delta\omega_H=\omega_H-\omega_H(1), \quad \epsilon_\perp=J_\perp/J.$$

We define the supermatrix $\mathbf{G}$,

$$\mathbf{G}=\begin{bmatrix}\mathbf{D}_N, & \mathbf{O}_N\\ \mathbf{B}_N, & \mathbf{I}_N\end{bmatrix}^{-1}=\begin{bmatrix}\mathbf{D}_N^{-1}, & \mathbf{O}_N\\ -\mathbf{B}_N\mathbf{D}_N^{-1}, & \mathbf{I}_N\end{bmatrix}. \quad (16)$$

Now, using Eq. (16) and (10), it follows that

$$(\mathbf{I}_N+\mathbf{G}_N{}^{(0)}\mathbf{\Delta D}_N)\mathbf{V}_N=0, \quad (17)$$
$$(-\mathbf{B}_N\mathbf{G}_N{}^{(0)}\mathbf{\Delta D}_N)\mathbf{V}_N+\mathbf{U}_N=0, \quad (18)$$

where $\mathbf{G}_N{}^{(0)}=\mathbf{D}_N^{-1}$. The elements of $\mathbf{G}_N{}^{(0)}$ can easily be constructed[4] with the result that

$$G_{m,n}{}^{(0)}=\frac{1}{2i\sin\theta}(e^{i(n+m)\theta}-e^{i|n-m|\theta}), \quad (19)$$

where $\theta$ is defined by Eq. (13) with the convention that the imaginary part of $\theta$ is positive. The surface-state eigenfrequencies are obtained by requiring the determinant of the coefficients to vanish:

$$|\mathbf{I}_N+\mathbf{G}_N{}^{(0)}\mathbf{\Delta D}_N|=0. \quad (20)$$

For the model we are considering, Eq. 20 yields

$$1-G_{11}{}^{(0)}\Delta d=0,$$

with

$$G_{11}{}^{(0)}=e^{i\theta}. \quad (21)$$

We note that in the RPA for $T>0$, the determination of the dispersion curves is a self-consistent problem, because of the functions $\langle S_z\rangle$ and $\langle S_z(1)\rangle$.

## III. DISPERSION CURVES AT $T=0$

Using Eqs. (13), (14), (15), (19), and (21) and setting $\theta=i\psi$, we find in units of $\omega_e$ that

$$e^\psi=(E-1-\omega_A)\times\left(\frac{2(\epsilon_\perp-1)}{\lambda_k^2}+\frac{\epsilon_\perp^2}{E-\omega_A-\epsilon_\perp/2+\delta}-\frac{1}{E-1-\omega_A}\right), \quad (22)$$

since $\epsilon_\perp{}^{(1)}=\epsilon_\perp$ at $T=0$. Here, $\delta$ equals $\Delta\omega_A+\Delta\omega_H$. Using the expression for $-2\cos\theta$, Eq. (13), we can also derive an expression for $e^\psi$ given by

$$e^\psi=A\pm(A^2-1)^{1/2}, \quad (23)$$

with

$$A=\frac{2[(1+\omega_A)^2-E^2]}{\lambda_k^2}-1. \quad (24)$$

The bulk solutions for zero propagation vector in the $x$ direction are given by setting $\psi=0$ in Eq. (23); thus, $A=1$. Equations (22) and (23) may be solved simultaneously to give a polynomial in $E$. However, because of the high degree of the resulting polynomial, except for $\epsilon_\perp=1$ or 0, the above expressions are most conveniently solved numerically by finding the intersections of Eq. (22) and (23) as a function of $E$ for a given choice of parameters. We describe the modes for ranges of the parameters $\epsilon_\perp$, $\omega_A$, and $\delta$ in the following subsections.

### A. Dispersion Curves for $\omega_A=\delta=0$

#### 1. $\epsilon_\perp=1$

The case $\epsilon_\perp=1$, as mentioned earlier, was discussed by Mills and Saslow. Since in this case it is possible to write a quadratic expression in $E$ for arbitrary values of $\omega_A$ and $\delta$, we proceed to do so even though in this subsection we restrict our discussion to $\omega_A=\delta=0$. We can write, for $\epsilon_\perp=1$,

$$(1+2\delta)E^2+\tfrac{1}{2}[(1+2\delta)^2-\lambda_k^2]E+\tfrac{1}{2}(1+\omega_A)[\lambda_k^2-1-2(1+2\delta)\omega_A+4\delta^2]=0. \quad (25)$$

Equation (25) reduces to Eq. (15) of Ref. 1 for $\lambda_k=1$. Now from Eq. (22), we also have that

$$e^\psi=\frac{1+2\delta}{1+2(\omega_A-\delta-E)}. \quad (26)$$

[4] N. Wax, *Noise and Stochastic Processes* (Dover Publications, Inc., New York, 1959), p. 301.

Equation (26) is equivalent to Eq. (10) of Ref. 1 for the values of $E$ equal to the eigenvalues of the surface spin waves. For $\delta=\omega_A=0$, we note immediately, from Eq. (26), that a negative-frequency branch cannot be allowed when $\epsilon_\perp=1$, since this would require that $\psi<0$. A plot of the solutions of Eq. (25) for $\delta=\omega_A=0$ is shown in Figs. 1 and 2 (curves labeled $\epsilon_\perp=1$). The slope at $\lambda_k=1$ is $1/\sqrt{2}$ of its bulk value. From Eq. (26), we further note that for small values of $E$ the amplitude of the surface mode decreases with depth approximately as $e^{-2nE}$ ($n=1, 2, \cdots$), where $n$ refers to the number of layers. On the other hand, at the end of the zone, $E$ approaches $\frac{1}{2}$ and $\psi\rightarrow\infty$ so that this mode (for which $\lambda_k\rightarrow 0$) is localized entirely at the surface.

### 2. $0\leqslant\epsilon_\perp<1$

As we mentioned in the Introduction, when $\epsilon_\perp$ is allowed to deviate from unity, a negative-frequency surface spin-wave branch appears. Negative frequencies

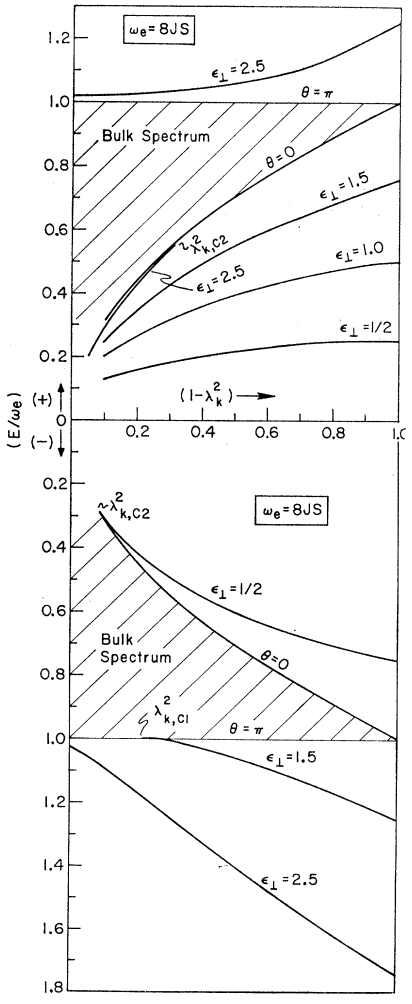


FIG. 1. Dispersion curves for $\pm E$ surface states as a function of $\lambda_k$. The shaded areas correspond to bulk states for values of $k_x$ between 0 and $\pi$ for a given value of $\lambda_k$. The abscissa is in units of $\omega_e$.

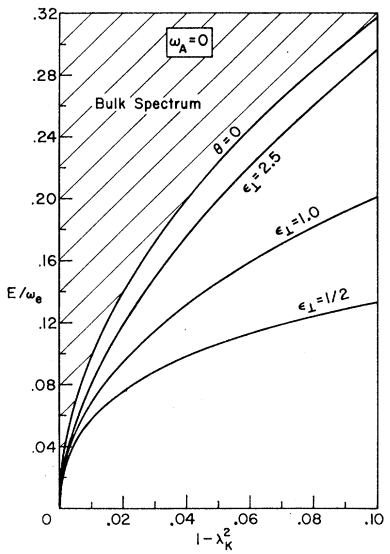


FIG. 2. Acoustical surface branch for $+E$ as a function of $\mathbf{k}$ for $\omega_A=0$. The curve labeled $\theta=0$ is the bulk curve for the zero propagation vector in the $x$ direction.

indicate right-hand circular polarization, while positive frequencies indicate left-hand circular polarization. In order to get physical insight into the origin of the $-E$ branch, we set $\epsilon_\perp=0$. This decouples the first layer from the crystal, and consequently should give a surface state now having a maximum on the second layer with the same characteristics as in the case of $\epsilon_\perp=1$, except for a change in its sense of precession. As in the case of $\epsilon_\perp=1$, we can write a quadratic in $E$:

$$E^2-\tfrac{1}{2}(1-\lambda_k^2)E-\tfrac{1}{2}(1+\omega_A)(1+2\omega_A-\lambda_k^2)=0 \quad (27)$$

and also,

$$e^{\psi}=-[(2/\lambda_k^2)(E-1-\omega_A)+1]. \quad (28)$$

For $\lambda_k=1$, we find that

$$E=\pm[\omega_A(1+\omega_A)]^{1/2} \quad (29)$$

Since $|E|>\omega_A$ according to Eq. (29), in contrast to the case $\epsilon_\perp=1$, only the negative frequency gives $\psi>0$. Now, as $\lambda_k\rightarrow 0$, at the end of the zone, we find on setting $\omega_A=0$ that $E\rightarrow-\frac{1}{2}$, and $\psi\rightarrow\infty$. The eigenvectors for this case show that the excitation amplitude is confined to the second layer of spins. Equation (27) is equivalent to Eq. (25) for negative $E$ when $\delta=0$. The above discussion gives a qualitative understanding of the origin of the negative-frequency branch which is illustrated in Fig. 1 for $0<\epsilon_\perp<1$. We note for $\epsilon_\perp$ greater than zero, the dispersion curve cuts off at

$$\lambda_k^2=2a-1/a^2\equiv\lambda_{k,C2}, \quad (30)$$

where

$$a=\frac{\epsilon_\perp^2-2}{(\epsilon_\perp+2)(\epsilon_\perp-1)}. \quad (31)$$

These cutoffs in the negative-surface branch occur at

the point, where the eigenvalue for the surface mode coincides with the bulk frequency. For values of $\lambda_k$ beyond that point no solution for real value of $E$ exist. The absence of a surface eigenstate beyond $\lambda_{k,C2}$ can be understood from Fig. 1. The shaded area indicates all of the possible bulk states. The frequency range for a given $\lambda_k$ is obtained by allowing $k_x$, the wave vector in the $x$ direction, to range over all of its values in the first Brillouin zone. A surface mode occurring within the shaded bulk continuum of state would decay into the corresponding bulk mode and hence would have a finite lifetime. The lifetime of such a mode would be approximately proportional to the density of continuum states at that energy and $\lambda_k$. From Eqs. (30) and (31), we note that if $\epsilon_\perp=0$ the cutoff is at $\lambda_{k,C2}=1$, as discussed earlier. As $\epsilon_\perp \to 1$ the cutoff approaches $\lambda_{k,C2}=0$.

On the other hand, the positive-frequency branch approaches zero frequency everywhere as $\epsilon_\perp \to 0$ for $\omega_A=0$. The slope at $\mathbf{k}=0$ is $1/\sqrt{2}$ of its bulk value independent of $\epsilon_\perp$.

### 3. $1<\epsilon_\perp<2$

The positive-frequency branch as indicated in Fig. 1 moves toward the bulk value as $\epsilon_\perp$ increases and exists for all values of $\lambda_k$. However, the negative-frequency branch is now restricted to lie above the bulk band (greater negative frequencies), and is cut off at

$$\lambda_{k,C1}{}^2=\frac{(\epsilon_\perp-1)(2+\epsilon_\perp)}{\epsilon_\perp{}^2}. \tag{32}$$

From Eq. (32) if $\epsilon_\perp<2$, $\lambda_{k,C1}<1$.

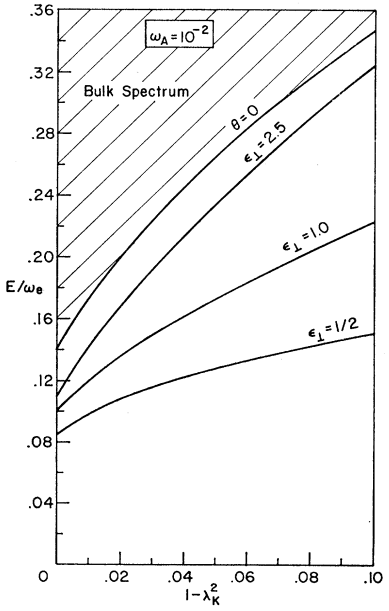


FIG. 3. Dispersion curves in the long wavelength limit for the $+E$ acoustical surface states for $\omega_A=10^{-2}$ and various values of $\epsilon_\perp$. The abscissa is in units of $\omega_e$.

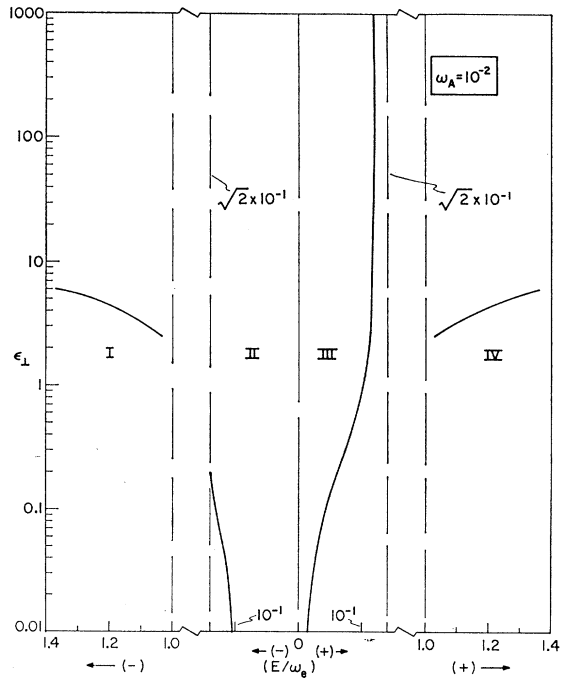


FIG. 4. Surface eigenvalue at $\lambda_k=1$ as a function of $\epsilon_\perp$ for $\omega_A=10^{-2}$. Note that the abscissa is a logarithmic scale and the ordinate is divided into four regions. Regions I and IV describe the optical mode lying above the bulk spectrum for $-E$ and $+E$, respectively, in units of $\omega_e$. Regions II and III show the $-E$ and $+E$ acoustical mode behavior.

### 4. $\epsilon_\perp \geqslant 2$

We note immediately from Eqs. (30) and (31) that for $\epsilon_\perp=2$ the $+E$ acoustic branch is cut off at $\lambda_{k,C2}=0$. However, one now obtains a $+E$ optical-frequency branch existing for all values of $\lambda_k$. This branch, for $\epsilon_\perp>2$, lies above the bulk spin-wave band as illustrated in Fig. 1. The eigenmode closely resembles the bulk mode at $k_x=\pi$, but is rapidly attenuated with increasing depth for values of $\epsilon_\perp$ greater than 2. For $\epsilon_\perp \geqslant 2$, the negative-frequency branch discussed earlier now exists for all values of $\lambda_k$. In Sec. IV, we will discuss the properties of these modes by investigating the form of their eigenvectors. The dispersion curves for the positive-frequency acoustical branch for $\lambda_k \sim 1.0$ (i.e., in the region about the origin of $\mathbf{k}$ space) are illustrated in Fig. 2.

## B. Dispersion Curves in the Long-Wavelength Limit for $\omega_A \neq 0$

In Fig. 3, we have sketched the dispersion curves for various values of $\epsilon_\perp$ and $\omega_A=10^{-2}$ (in units of $\omega_e$). As noted by Mills and Saslow, at $\mathbf{k}=0$ the frequency for the acoustical branch is relatively insensitive to changes in $\epsilon_\perp$ provided $\omega_A \ll \omega_e$. Their conclusions were based upon a perturbation calculation valid for small changes in $\epsilon_\perp$. We show in Figs. 4 and 5, the behavior of the frequency at $\mathbf{k}=0$ for arbitrary changes in $\epsilon_\perp$. The graphs are separated into four sections in order to indicate

clearly the various points mentioned earlier in connection with Fig. 1. The center portions of the graphs give the dependence of the acoustical frequency on $\epsilon_\perp$, while the outermost sections illustrate the dependence of the optical frequencies on $\epsilon_\perp$. In Fig. 4 we have taken $\omega_A = 10^{-2}$. We note first that for $\epsilon_\perp = 1$, the frequency is equal to $\sqrt{10^{-2}} = 0.1$, as given by the quadratic equation discussed earlier. Region III of Fig. 4 shows the dependence of the positive-acoustical branch as $\epsilon_\perp$ deviates from unity. We note that for $\epsilon_\perp > 1$, the frequency at $\mathbf{k}=0$ is even less sensitive to changes in $\epsilon_\perp$ than that suggested by the perturbation calculation of Mills and Saslow, and approaches, in the limit $\epsilon_\perp \to \infty$ the bulk value of $\sqrt{2}\times 10^{-1}$. On the other hand, for $\epsilon_\perp \to 0$, the frequency approaches $10^{-2}$. The unsymmetrical dependence of the frequency on $\epsilon_\perp$ about unity can be understood simply as follows: As the surface mode approaches its bulk value, $\Psi$ decreases, therefore, more layers of spins participate in the eigenmode, so that a perturbation at the surface becomes relatively less important. However, as $\epsilon_\perp \to 0$, $\psi$ increases, and consequently the surface perturbation gives a larger frequency shift until finally no surface mode with positive frequency exists at $\epsilon_\perp = 0$. In region II, we show the behavior of the negative-frequency branch which at $\epsilon_\perp = 0$ has a frequency equal to $10^{-1}$. This branch has a cutoff at $\mathbf{k}=0$, depending on the values of $\omega_A$ and $\epsilon_\perp$. Recall that if $\omega_A$ is zero, we have no negative-frequency solution at $\mathbf{k}=0$ unless $\epsilon_\perp = 0$. Regions I and IV show the behavior of the optical branch for $\epsilon_\perp \gtrsim 2$ which as indicated in the figure are very sensitive to changes in $\epsilon_\perp$. In the discussion so far, we have restricted our consideration

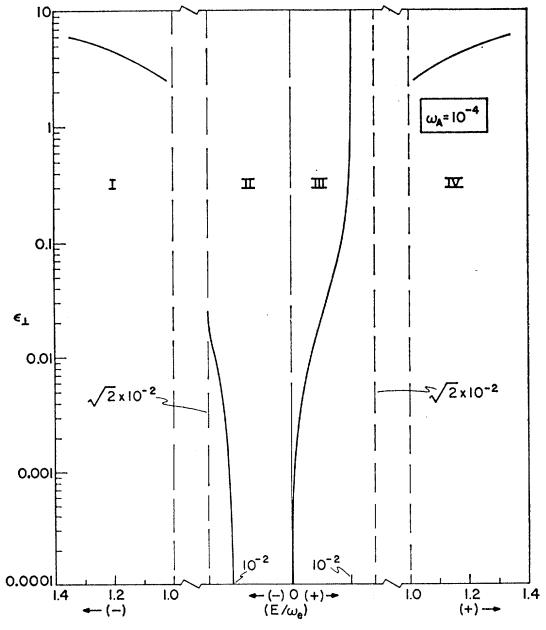


FIG. 5. Surface eigenvalue at $\lambda_\mathbf{k}=1$ as a function of $\epsilon_\perp$ for $\omega_A = 10^{-4}$. The abscissa is a logarithmic scale and the four regions have the same meaning as in Fig. 3.

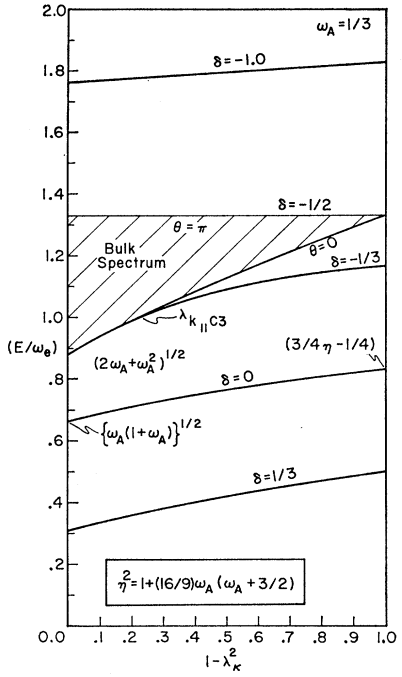


FIG. 6. Dispersion curves for $\epsilon_\perp = 1$ as a function of $\lambda_\mathbf{k}$ for various value of $\delta$ in units of $\omega_e$. As indicated in the figure, $\omega_A = \frac{1}{3}$.

to the case where $\omega_A$ is small and concluded that the positive-acoustical branch is relatively insensitive to deviations of $\epsilon_\perp$ from unity. Furthermore, in agreement with the perturbation calculation of Mills and Saslow, the mode is found also to be insensitive to changes in $\delta$. A similar plot is given for $\omega_A = 10^{-4}$ in Fig. 5. However, the above conclusions are drastically modified if $\omega_A$ is of the order of $\omega_e$.

In Sec. IV, we discuss this case for $\epsilon_\perp = 1$ and changes in $\delta$.

### C. $\varepsilon = 1$; $\omega_A \simeq \omega_e$

In this subsection we discuss briefly the case when $\omega_A$ is on the order of $\omega_e$. This case is of physical interest, since certain crystals are known to have such characteristics. The compound $FeF_2$, for example, has $\omega_A \sim \frac{1}{3}\omega_e$. To illustrate the drastic dependence of the surface branches on the surface parameters for this case, in Fig. 6 we have plotted the surface eigenvalues as a function of $\mathbf{k}$ for various values of $\delta = \Delta\omega_H + \Delta\omega_A$. Even for $\epsilon_\perp = 1$, we note that the acoustical branch exhibits cutoffs at

$$\lambda_{\mathbf{k},C3} = [1+2\omega_A(1+2\delta)-4\delta^2]^{1/2} \qquad (33)$$

for negative values of $\delta$. (For negative $\delta$, the anisotropy field at the surface is larger than its bulk value.) The maximum positive value that $\delta$ can have is $\omega_A$ which corresponds to zero anisotropy on the first layer. For $\delta = -\frac{1}{2}$ [see Eq. (25)], we have an optical branch which has an energy equal to $1+\omega_A$ for all values of $\mathbf{k}$. The expression for $\eta$ defined in Fig. 6 differs from that of

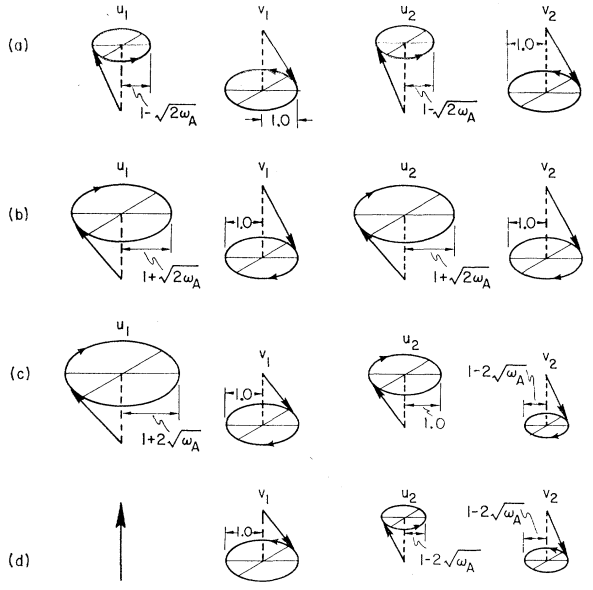


FIG. 7. The amplitude of the first four layers of the eigenvectors. Increasing depth is from left to right. (a) Bulk eigenvectors for $k_x=\mathbf{k}=0$ and $E=-(2\omega_A)^{1/2}$. (b) Bulk eigenvectors for $k_x=\mathbf{k}=0$ and $E=(2\omega_A)^{1/2}$. (c) Surface eigenvectors for $k=0$, $E=\sqrt{\omega_A}$, $\epsilon_\perp=1.0$. (d) Surface eigenvectors for $\mathbf{k}=0$, $E=-\sqrt{\omega_A}$, $\epsilon_\perp=0.0$.

Mills and Saslow. The discrepancy is attributed to an algebraic error in their paper.

## IV. EIGENVECTORS FOR SPECIAL POINTS IN THE BRILLOUIN ZONE

Here, we illustrate the behavior of the eigenvectors along the $x$ direction for $\lambda_k=1$. We normalize the eigenvectors by taking $v_1=1$ and then, using Eqs. (17) and (18), we obtain

$$\begin{aligned} v_l &= G_{l,1}\Delta d, \\ u_l &= \frac{\lambda_k v_l(e^{\psi}+1)}{2[E-(1+\omega_A)]}, \quad l\neq 1 \\ u_1 &= \frac{\epsilon_\perp \lambda_k}{2[E-(1+\omega_A)+d_{11}]}. \end{aligned} \tag{34}$$

Using Eqs. (3), (6), and (7), we define

$$\begin{aligned} S_{l,x}{}^{(b)}(\mathbf{k},E',t)+iS_{l,y}{}^{(b)}(\mathbf{k},E',t) &= e^{i\mathbf{k}\cdot\rho_l}e^{-iE't}v_l{}^{(\mathbf{k},E')}, \\ S_{l,x}{}^{(a)}(\mathbf{k},E',t)+iS_{l,y}{}^{(a)}(\mathbf{k},E',t) &= e^{i\mathbf{k}\cdot\rho_l}e^{-iE't}u_l{}^{(\mathbf{k},E')}. \end{aligned} \tag{35}$$

Equations (35) can be illustrated graphically by drawing a circle of radius $A_l$ equal to $|v_l|$ or $|u_l|$. At $t=0$ and $\rho_l=0$, the phase $\phi_l=\tan^{-1}(S_{l,y}/S_{l,x})$ is either 0 or $\pi$. The bulk states at $\mathbf{k}=0$ and $k_x=0$ for positive and negative $E$ are illustrated in Figs. 7(a) and 7(b). The direction of the arrow on the circle indicates the direction of spin precession according to Eq. (35) for $t\neq 0$ and $\rho_l=0$. We note that the maximum amplitude for negative $E$ is on the ($b$) sublattice, while for positive $E$ the amplitude is a maximum on the ($a$) sublattice. This property remains at finite $\mathbf{k}$.

In Figs. 7(c) and 7(d), we show the surface eigenvectors at $\mathbf{k}=0$. Figure 7(c) is for the $+E$ branch for $\epsilon_\perp=1$ (no negative branch is allowed). The amplitude falls off with increasing depth into the crystal and is maximum on the first layer. To illustrate the negative branch, we show the extreme case of $\epsilon_\perp=0$ in Fig. 7(d). Here the amplitude is a maximum on the second layer while the first layer is completely decoupled. With $0<\epsilon_\perp<1$, both positive and negative branches can occur. The amplitude decreases exponentially with distance into the crystal on each successive spin-up layer but not on the spin-down layers. As discussed earlier for $\epsilon_\perp\gtrless 2$ new states are allowed at $\mathbf{k}=0$. For $\epsilon_\perp=2$, $E=\pm 1$ are solutions of the eigenvalue surface equation. The mode for $E=1$ has an infinite amplitude on the ($a$) sublattice because of our normalization of $v_1$, this can be seen from Eq. (34), for $\omega_A=0$. This mode actually was obtained by setting $\epsilon_\perp=2+\delta_\perp$ and allowing $\delta_\perp\to 0$. For $\delta_\perp=0$, these modes have the same characteristics as the bulk mode for $k_x=\pi$. However, only for $\delta_\perp=0$ are these modes undamped with depth into the crystal. Since the $E=+1$ mode has an amplitude increasing with decreasing $\delta_\perp$, we have chosen, for this case, $v_1$ to be proportional to $\delta_\perp$ so that $u_1$ is normalized to unity. In Table I, we give the phase an amplitude of the optical modes at $\lambda_k=1$ and identify them with the bulk modes for $k_x=\pi$ and $\lambda_k=1$. The modes at the end of the zone for which $E=+\frac{1}{2}\epsilon_\perp$ and $E=-\frac{1}{2}(\epsilon_\perp+1)$ are identified

TABLE I. $A$ is the amplitude of the spin precessional circle. The radius of the circle is given by $(S_x{}^2+S_y{}^2)^{1/2}$. The phase angle $\phi$ is defined as $\phi=\tan^{-1}(S_y/S_x)$. The amplitude $A(\lambda_k=1,\ k_x=\pi,\ E=\pm 1)$ refers to bulk states, and $A(\lambda_k=1,\ \epsilon_\perp=2,\ E=\pm 1)$ are the surface-state amplitudes. The same indexing applies to the phase $\phi$.

| | $u_1{}^{(a)}$ | $v_1{}^{(b)}$ | $u_2{}^{(a)}$ | $v_2{}^{(b)}$ | $u_3{}^{(a)}$ | $v_3{}^{(b)}$ | $u_4{}^{(a)}$ | $v_4{}^{(b)}$ |
|---|---|---|---|---|---|---|---|---|
| $A(\lambda_k=1,\ k_x=\pi,\ E=1)$ | 1 | 0 | 1 | 0 | 1 | 0 | 1 | 0 |
| $A(\lambda_k=1,\ \epsilon_\perp=2,\ E=1)$ | 1 | 0 | 1 | 0 | 1 | 0 | 1 | 0 |
| $\phi(\lambda_k=1,\ k_x=\pi,\ E=1)$ | $\pi$ | $\pi$ | 0 | 0 | $\pi$ | $\pi$ | 0 | 0 |
| $\phi(\lambda_k=1,\ \epsilon_\perp=2,\ E=1)$ | $\pi$ | $\pi$ | 0 | 0 | $\pi$ | $\pi$ | 0 | 0 |
| $A(\lambda_k=1,\ k_x=\pi,\ E=-1)$ | 0 | 1 | 0 | 1 | 0 | 1 | 0 | 1 |
| $A(\lambda_k=1,\ \epsilon_\perp=2,\ E=-1)$ | 0 | 1 | 0 | 1 | 0 | 1 | 0 | 1 |
| $\phi(\lambda_k=1,\ k_x=\pi,\ E=-1)$ | $\pi$ | $\pi$ | 0 | 0 | $\pi$ | $\pi$ | 0 | 0 |
| $\phi(\lambda_k=1,\ \epsilon_\perp=2,\ E=-1)$ | $\pi$ | $\pi$ | 0 | 0 | $\pi$ | $\pi$ | 0 | 0 |

with $\lambda_{\mathbf{k}}=0$ and $E=\pm 1$ of the bulk spectrum. These surface modes are highly attenuated for $\epsilon_1 \neq 2$ or 1, and in fact they exist only on the first layer for $+E$ and on the second layer for $-E$ at $\lambda_{\mathbf{k}} \equiv 0$.

## V. CONCLUSIONS AND DISCUSSION

In the preceding sections, we have examined the dependence of the spin-wave spectrum and eigenvectors on arbitrary changes in the exchange constant and anisotropy energy at the surface. As discussed by Mills and Saslow, when the exchange at the surface is taken to be equal to its bulk value, one surface branch exists having its maximum energy equal to $\frac{1}{2}$ of its bulk value and its minimum value equal to $1/\sqrt{2}$ of its bulk value for small values of the bulk anisotropy. This mode at $\mathbf{k}=0$ is found not to be sensitive to changes in $\epsilon_1$ and $\delta$, provided $\omega_A$ is small. On the other hand, for $\omega_A \sim \omega_e$ we have shown in Fig. 6 that even when $\epsilon_1=1$, the acoustical branch is cut off for small values of $\mathbf{k}$ if $\delta$ is negative (an increase in the anisotropy energy on the surface). Furthermore, an optical branch above the bulk spectrum exists if $\delta \leqslant -\frac{1}{2}$. For values of $\epsilon_1$ differing from unity and for arbitrary values of $\omega_A$, three surface branches can exist. In the region $0 \leqslant \epsilon_1 \leqslant 1$, a $+E$ acoustical branch extends over the entire domain of $\mathbf{k}$. This branch is a generalization of the branch discussed by Mills and Saslow for $\epsilon_1=1$. For this mode, the amplitude is a maximum on the first layer and decreases with depth into the crystal. In addition to this $+E$ branch we find a $-E$ branch (for $\epsilon_1 \neq 1$) which does not exist for all values of $\mathbf{k}$, except for $\epsilon_1=0$ and $\omega_A=0$. If $\omega_A \neq 0$ this branch can exist over all values of $\mathbf{k}$ for values of $\epsilon_1$ different from zero. In contrast to the $+E$ mode, this mode has its maximum excitation amplitude on the second layer.

When $1<\epsilon_1<2$ the surface acoustical branch with $+E$ still exists for all $\mathbf{k}$ and approaches the bulk branch as $\epsilon_1 \rightarrow 2$. In addition, we find an optical $-E$ branch which cuts off for small values of $\mathbf{k}$. The negative-acoustical branch does not exist for this range of $\epsilon_1$. When $\epsilon_1 \geqslant 2$ we have three branches. The $+E$ acoustical branch which truncates for large values of $\mathbf{k}$ and two optical branches extending over all values of $\mathbf{k}$. The cutoffs in the surface branches can be physically understood by noting that no surface mode for real $E$ can exist in the bulk continuum lying between $k_x=0$ and $k_x=\pi$ for a given value of $\lambda_{\mathbf{k}}$. Since the one-dimensional Green's function in that region has an imaginary part, Eq. (22) cannot be satisfied for real $E$. However, virtual states can exist in this region but since the one dimensional density of states is very large except at $k_x=0$ and $k_x=\pi$ these modes are rapidly attenuated in time.

At the cutoff values of $\Lambda_q$ it can be shown that the surface branch meets the bulk continuum tangentially. If the branch is continued beyond $\Lambda_q$ the surface branch continuously moves away from the bulk continuum. These solutions, however, can be shown to be unphysical in that they correspond to waves which grow with increasing depth into the crystal. On the other hand, if one adopts the point of view commonly used in continuum theory, i.e., to equate the real part of the eigenvalue equation to zero, then solutions of the surface eigenvalue equation can be extended into the continuum. These solutions correspond to virtual states with a lifetime determined by the imaginary part of the Green's function. It is found that the surface branch continuously extends into the bulk continuum but exhibits a discontinuity in slope at the cutoff values of $\Lambda_q$.

As a final remark, we point out that the frequency of the acoustical-surface branch at $\mathbf{k}=0$ is very sensitive to geometry. Any other principal surface of the bcc contains both spins of both sublattices. We find, in this case, that for reasonable values of the exchange parameters and for small values of $\omega_A$ the $\mathbf{k}=0$ mode lies at its bulk value. The basic equations given in a previous publication[2] for the simple cube cut along the {100} surface can be used to describe the {110} surface of the bcc crystal provided the parameters of the cubic equation are redefined.

## ACKNOWLEDGMENT

The authors are grateful to M. Sparks for pointing out an algebraic mistake in Eq. (34). The corrections have been made in this paper.